ELSEVIER

Journal of Nuclear Materials 240 (1997) 196–204

journal of nuclear materials

Defect production considerations for gamma ray irradiation of reactor pressure vessel steels [1]

Dale E. Alexander *

Materials Science Division, Argonne National Laboratory, Argonne, IL 60439, USA

Received 30 May 1996; accepted 16 October 1996

Abstract

Motivated by the recent interest in gamma ray embrittlement of nuclear reactor pressure vessels (RPVs), calculations were performed to evaluate aspects of defect production by gammas in iron and steel. In addition to determining displacement damage cross-sections, the atomic recoil energy dependence of gamma-induced defect production was described by integral recoil damage spectra, $W(T)$, and their associated median recoil damage energies, $T_{1/2}$. These latter characterizations, should be particularly useful in evaluating the contribution of gamma ray generated defects to microstructural changes causing radiation embrittlement. The results for monoenergetic gammas, as well as for gamma rays with a spectrum of energies characteristic of a RPV, reveal $T_{1/2}$ values of < 100 eV, about three orders of magnitude smaller than for fast-neutrons, the radiation of primary concern in previous embrittlement studies. The relative contributions of various gamma interactions to defect production, as well as the role of light alloy element-induced secondary displacement mechanisms, are also considered.

1. Introduction

Gamma rays have been used extensively to study a variety of radiation effects in materials susceptible to ionization damage. The typically high electronic conductivities of metals and metallic alloys, however, preclude any appreciable effect from such ionization damage. Nonetheless, gamma rays can induce atomic displacements in metals, a fact recognized early in the study of radiation effects [1]. The highly penetrating nature of gamma rays has been exploited in experiments measuring changes in sensitive bulk material properties such as elastic modulus and resistivity of metals and alloys [2,3].

There is renewed interest in gamma ray damage in metals, prompted by a need to understand its impact on radiation-induced embrittlement of ferritic nuclear reactor pressure vessel (RPV) steels [4–9]. While this field has long been dominated by concerns of fast neutron (energies > 0.1 MeV) damage effects, recent studies have indicated that in certain reactor designs, gamma rays can contribute a significant fraction of the displacements per atom (dpa) in RPVs (see Table 1), and thus may figure importantly in radiation embrittlement. Such analyses however, are complicated by the lack of experimental data on gamma ray displacement damage cross-sections for Fe and steels, dictating a reliance on calculations and accompanying uncertainties.

Aside from accurately determining the magnitude of displacement damage cross-sections and absolute dpa rates, evaluating the contribution of gamma rays to embrittlement requires consideration of the nature of gamma ray defect production relative to that of fast-neutron irradiation. Unlike fast-neutrons, the kinematics of gamma ray interactions are such that they tend to produce very low-energy atomic recoils. Molecular dynamic computer simulations have shown that significant differences in nascent defect production result between low- and high-energy atomic recoils in metals [12,13]. Experimentally, such

* Tel.: +1-630 252 7783; fax: +1-630 252 4798.

[1] Work supported by the U.S. Department of Energy, BES-Materials Sciences, under contract #W-31-109-ENG-38 with Argonne National Laboratory. The U.S. Government retains a nonexclusive, royalty-free license to publish or reproduce the published form of this contribution, or allow others to do so, for U.S. Government purposes.

PII S0022-3115(96)00713-1

Table 1
Calculated displacement damage rates generated by various sources at the quarter thickness location of the general electric advanced boiling water reactor (ABWR)

Displacement damage source	Damage rate (dpa/s)
Gamma rays	1.0×10^{-13}
Neutrons	2.0×10^{-13}
Thermal neutron (n, γ) recoils	3.5×10^{-16}

Gamma results take from analysis in Ref. [6]. Neutron results determined from SPECTER calculations [10,11]. Entry for 'neutrons' includes damage from neutrons of all energies.

recoil energy differences are known to have important consequences on microstructural phenomena such as segregation [14] and diffusion [15]. Since mechanical properties are intimately related to material microstructure, understanding low energy recoil effects is essential for understanding and predicting mechanical property changes due to gamma rays. Providing a comparative basis for describing differences in recoil spectra for varying irradiation environments (e.g., gamma rays versus fast-neutrons) which can be correlated with an effect on microstructural evolution is therefore desirable.

These differences may be characterized through comparison of integral recoil damage spectra, $W(T)$ [16,17]. This function, also known as the 'weighted average' recoil spectrum, gives the integral fraction of displacement damage produced by recoils with energies less than or equal to the primary recoil energy, T. It has a value of zero just below the minimum threshold displacement energy of a material, T_d, and a value of unity at the maximum atomic recoil energy, T_{max}, produced by a given irradiation. In part, this function provides a 'picture' of the range in recoil energies over which displacement damage is generated by the irradiating particles.

Although it would be useful for comparative purposes, as elaborated by previous authors [5,16,17], no single parameter completely and uniquely embodies the information present in the function $W(T)$. However, one approach that has been commonly adopted is to characterize the $W(T)$ spectrum by its median recoil damage energy, $T_{1/2}$. This parameter is the recoil energy at which $W(T) = 0.5$, i.e., one-half of the displacement damage is produced by recoils with energies above and below $T_{1/2}$. As such it provides a measure of the recoil spectrum 'hardness' for a given irradiation and is thus a useful comparative metric to help assess experimental results.

In this paper, calculations are presented for damage cross-sections, integral recoil damage spectra and median recoil damage energies in iron produced by monoenergetic gamma rays, as well as a 'typical' energy spectrum of gamma rays present in a RPV; the latter is of particular interest to radiation embrittlement evaluations. Additional consideration is given to secondary displacement damage effects resulting from, for example, carbon recoils in steel. As a whole, these results provide a basis for interpretation of experiments evaluating the role of gamma generated defects in the embrittlement of ferritic steels.

2. Calculations

The integral recoil damage spectrum is defined generally as

$$W(T) = \frac{\int_{E_{\gamma,\min}}^{E_{\gamma,\max}} \phi(E_\gamma)\,\mathrm{d}E_\gamma \int_{T_d}^{T} \left(\mathrm{d}\sigma_\gamma(E_\gamma, T')/\mathrm{d}T'\right) \upsilon(T')\,\mathrm{d}T'}{\int_{E_{\gamma,\min}}^{E_{\gamma,\max}} \phi(E_\gamma)\,\sigma_\gamma(E_\gamma)\,\mathrm{d}E_\gamma} \quad (1)$$

where $\phi(E_\gamma)$ = the energy dependent gamma flux, $\mathrm{d}\sigma_\gamma(E_\gamma, T')/\mathrm{d}T'$ = the differential cross-section for a gamma of energy E_γ to produce a recoil atom with energy T', $\upsilon(T')$ = the damage function, i.e., the average number of displacements generated by a primary recoil of energy T', T_d = the atomic displacement threshold of the material, $E_{\gamma,\max}$ = the maximum gamma energy present in the spectrum, $E_{\gamma,\min}$ = the minimum gamma energy capable of inducing a permanent atomic displacement and $\sigma_\gamma(E_\gamma)$ = the total damage cross-section per atom for a gamma ray of energy E_γ.

The total damage cross-section is defined as

$$\sigma_\gamma(E_\gamma) = \int_{T_d}^{T_{max}(E_{max})} \frac{\mathrm{d}\sigma_\gamma(E_\gamma, T')}{\mathrm{d}T'} \upsilon(T')\,\mathrm{d}T', \quad (2)$$

where the integration is performed to the maximum recoil energy, $T_{max}(E_{max})$, which is determined by the nature of the gamma interaction as further described below.

Damage cross-section calculations, as defined by Eq. (2), have been previously performed for gamma rays by Oen and Holmes [18], Dienes and Vineyard [19], Baumann [9] and Rehn and Birtcher [4]. The critical distinction between the present work and these previous damage calculations is that the determination of $W(T)$ (and hence $T_{1/2}$) in the present study, evaluates the integration in the numerator of Eq. (1) at a sufficient number of specific recoil energies to provide an accurate assessment of its functional dependence.

Two simplifications of Eq. (1) are made for use in subsequent calculations. First, for a monoenergetic gamma source, integration over the gamma ray energy is eliminated and $W(T)$ reduces to

$$W_{MONO}(T) = \frac{\int_{T_d}^{T} \left(\mathrm{d}\sigma_\gamma(E_\gamma, T')/\mathrm{d}T'\right) \upsilon(T')\,\mathrm{d}T'}{\sigma_\gamma(E_\gamma)}. \quad (3)$$

A second simplification recognizes that calculated or mea-

sured nuclear reactor gamma flux energy spectra are typically expressed in discretized forms with constant gamma fluxes assigned to gamma energy bins (see Fig. 1). Hence, the integration over gamma energy in Eq. (1) may be discretized to give

$$W_{\mathrm{SPEC}}(T) = \frac{\sum_{i=1}^{i_{\max}} \phi_i \int_{T_d}^{T} \left(\mathrm{d}\sigma_\gamma(E_{\gamma,i}, T')/\mathrm{d}T'\right) \upsilon(T')\,\mathrm{d}T'}{\sum_{i=1}^{i_{\max}} \phi_i \sigma_\gamma(E_{\gamma,i})}, \quad (4)$$

where ϕ_i is a constant gamma flux for the ith energy bin, of width ΔE_γ, defined by

$$\phi_i \equiv \phi(E_{\gamma,i}) = \int_{E_{\gamma,i}-\frac{1}{2}\Delta E_\gamma}^{E_{\gamma,i}+\frac{1}{2}\Delta E_\gamma} \phi(E'_\gamma)\,\mathrm{d}E'_\gamma. \quad (5)$$

In the remainder of the spectral calculations, the energy bin subscript 'i' is omitted for clarity.

2.1. Primary displacement damage

Evaluation of $W(T)$ and $\sigma_\gamma(E_\gamma)$ requires identifying the form of the differential cross-section, $\mathrm{d}\sigma_\gamma(E_\gamma, T')/\mathrm{d}T'$, which in turn depends on the mechanism of atomic recoil production. Gamma rays generate recoils indirectly, primarily through the production of energetic particles which subsequently displace lattice atoms. The calculations presented here focus exclusively on those gamma interactions generating electrons: the photoelectric effect (PE), Compton scattering (CS), and pair production (PP) [20]. Although photonuclear reactions such as (γ, n) are capable of producing damage above gamma threshold energies of about 11 MeV in iron, the magnitude of displacements from these interactions are negligible for the energies and fluxes of interest here (i.e., gamma energy spectra in RPVs) [5,6].

Assuming the dimensions of the material are large with respect to the range of electrons generated via the three

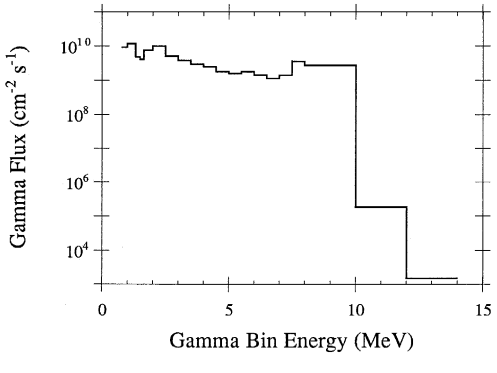

Fig. 1. Discretized gamma ray energy spectrum at the quarter-thickness ($\frac{1}{4}T$) location of the advanced boiling water reactor (ABWR) pressure vessel [6].

gamma interactions, Eqs. (3) and (4) may be expressed in more detail as follows. For a monoenergetic gamma source,

$$W_{\mathrm{MONO}}(T) = \int_{E_{\min}}^{E_{\max,k}} \left[\frac{\mathrm{d}\sigma_{\mathrm{PE}}(E_\gamma, E)}{\mathrm{d}E} + \frac{\mathrm{d}\sigma_{\mathrm{CS}}(E_\gamma, E)}{\mathrm{d}E} + 2\frac{\mathrm{d}\sigma_{\mathrm{PP}}(E_\gamma, E)}{\mathrm{d}E} \right] \left(\sigma_{\gamma,\mathrm{PE}}(E_\gamma) + \sigma_{\gamma,\mathrm{CS}}(E_\gamma) + \sigma_{\gamma,\mathrm{PP}}(E_\gamma)\right)^{-1} \int_{E_{\min}}^{E} \frac{N_{\mathrm{A}}}{-\mathrm{d}E'/\mathrm{d}x} \int_{T_d}^{T} \frac{\mathrm{d}\sigma_{\mathrm{e}}(E', T')}{\mathrm{d}T'} \times \upsilon(T')\,\mathrm{d}T'\,\mathrm{d}E'\,\mathrm{d}E, \quad (6)$$

and for a discretized gamma ray spectrum,

$$W_{\mathrm{SPEC}}(T) = \sum_{i=1}^{i_{\max}} \phi_i \int_{E_{\min}}^{E_{\max,k}} \left[\frac{\mathrm{d}\sigma_{\mathrm{PE}}(E_\gamma, E)}{\mathrm{d}E} + \frac{\mathrm{d}\sigma_{\mathrm{CS}}(E_\gamma, E)}{\mathrm{d}E} + 2\frac{\mathrm{d}\sigma_{\mathrm{PP}}(E_\gamma, E)}{\mathrm{d}E} \right] \times \left(\sum_{i=1}^{i_{\max}} \phi_i \left[\sigma_{\gamma,\mathrm{PE}}(E_\gamma) + \sigma_{\gamma,\mathrm{CS}}(E_\gamma) + \sigma_{\gamma,\mathrm{PP}}(E_\gamma) \right] \right)^{-1} \int_{E_{\min}}^{E} \frac{N_{\mathrm{A}}}{-\mathrm{d}E'/\mathrm{d}x} \int_{T_d}^{T} \frac{\mathrm{d}\sigma_{\mathrm{e}}(E', T')}{\mathrm{d}T'} \upsilon(T')\,\mathrm{d}T'\,\mathrm{d}E'\,\mathrm{d}E, \quad (7)$$

where $\mathrm{d}\sigma_k(E_\gamma, E)/\mathrm{d}E$ = the differential cross-section for a gamma of energy E_γ to produce an electron of energy E via gamma interaction 'k' where k = PE, CS or PP. The factor of 2 preceding the PP term accounts for the damage generated by both the positron and electron produced via this interaction. N_{A} = atomic density of the target, $-\mathrm{d}E'/\mathrm{d}x$ = the linear energy loss experienced by an electron of energy E', $\mathrm{d}\sigma_{\mathrm{e}}(E', T')/\mathrm{d}T'$ = the differential cross-section for an electron of energy E' to produce a recoil atom of energy T', $E_{\min}$ = the minimum electron energy capable of producing a permanent displacement, $E_{\max,k}$ = the maximum electron energy generated via gamma interaction 'k', where k = PE, CS, PP, and $\sigma_{\gamma,k}(E_\gamma)$ = the damage cross-sections for each gamma interaction 'k'.

Similarly, the damage cross-section for each 'k' interaction is expressed more specifically as

$$\sigma_{\gamma,k}(E_\gamma) = \int_{E_{\min}}^{E_{\max,k}} n \frac{\mathrm{d}\sigma_k(E_\gamma, E)}{\mathrm{d}E} \int_{E_{\min}}^{E} \frac{N_{\mathrm{A}}}{-\mathrm{d}E'/\mathrm{d}x} \int_{T_d}^{T_{\max}(E_{\max,k})} \frac{\mathrm{d}\sigma_{\mathrm{e}}(E', T')}{\mathrm{d}T'} \times \upsilon(T')\,\mathrm{d}T'\,\mathrm{d}E'\,\mathrm{d}E, \quad (8)$$

where $n = 1$ for k = PE and CS and $n = 2$ for k = PP

(again, the factor of 2 for PP accounts for damage from both the gamma generated positron and electron). The *total* gamma damage cross-section per atom, $\sigma_{\gamma,k}(E_\gamma)$, is simply the sum of the damage cross-sections for the 'k' interactions,

$$\sigma_\gamma(E_\gamma) = \sigma_{\gamma,\mathrm{PE}}(E_\gamma) + \sigma_{\gamma,\mathrm{CS}}(E_\gamma) + \sigma_{\gamma,\mathrm{PP}}(E_\gamma). \quad (9)$$

The maximum atomic recoil energy used as an integration limit in Eq. (8) is a function of the maximum electron kinetic energy generated by gamma interaction 'k', $E_{\max,k}$, and is expressed in relativistic form as

$$T_{\max}(E_{\max,k}) = \frac{2m_e}{M}\left(\frac{E_{\max,k} + 2m_e c^2}{m_e c^2}\right)E_{\max,k}, \quad (10)$$

where m_e is the mass of the electron, M is the mass of the target atom, and $m_e c^2$ is the rest energy of an electron (0.511 MeV). The minimum electron energy, $E_{\min}$, which appears as a lower integration limit in the Eqs. (6)–(8), is found by solving Eq. (10) for $E_{\min}$ after replacing $T_{\max}(E_{\max,k})$ with T_d and $E_{\max,k}$ with $E_{\min}$.

The integrals over T' and E' in Eqs. (6)–(8) represent the average number of displacements produced during the slowing of each gamma-generated electron of energy E. Relativistic expressions used in this part of these equations are the same as those used by Oen and Holmes [18] in their damage cross-section calculations. The McKinley–Feshbach differential cross-section, which is an approximate form of the exact Mott series differential cross-section applicable for targets with $Z \le 29$ [21,22], was used for $(\mathrm{d}\sigma_e(E', T')/\mathrm{d}T')$. The Bethe–Ashkin relativistic formula for the average linear energy loss, $-\mathrm{d}E'/\mathrm{d}x$, due to electronic excitation was used with an ionization potential for Fe of $I = 336$ eV [23].

The standard modified Kinchin–Pease damage function [24],

$$\upsilon(T') = \begin{cases} 0 & T' < T_d \\ 1 & T_d \le T' < 2.5T_d \\ 0.8\dfrac{T'}{2T_d} & T' \ge 2.5T_d \end{cases}, \quad (11)$$

was used as well as the standard displacement threshold energy, T_d, for Fe of 40 eV [24]. It was further assumed that all the recoil energy, T', contributes to defect production, thus ignoring any electronic energy loss by the recoil atoms. This will tend to overestimate the damage cross-section but should have a minimal effect on calculated $W(T)$ spectra.

Expressions for the differential cross-sections for the photoelectric effect, Compton scattering, and pair production interactions used in Eqs. (6)–(8) are provided in Refs. [25–27], respectively.

2.2. Secondary displacement damage

Light elements in alloys, such as carbon in a RPV steel, can reduce the lower energy limit for gamma ray damage production. This phenomenon was observed previously in the case of electron irradiation of Pt–C alloys [28]. Gamma rays which do not have sufficient energy to produce an Fe displacement directly in the steel via the three interactions described above may instead do so *indirectly* first through the displacement of lighter carbon atoms. The recoiling carbon atoms more effectively transfer energy to the Fe atoms than the gamma-generated electrons and thus are kinematically capable of displacing the Fe atoms in circumstances where the direct electron–Fe interactions cannot. Hence defects can be generated in an RPV steel below the threshold gamma energy necessary to produce displacements in pure Fe (i.e., secondary displacement damage).

In order to evaluate the significance of secondary displacements, the total damage cross-section (per *target* atom) for the process was evaluated for an Fe–1 at.% C alloy and compared with that determined for the direct process (i.e., essentially as described by Eqs. (8) and (9)) in the alloy. For monoenergetic gamma irradiation, the total secondary displacement damage cross-section per target atom is defined as

$$\sigma_\gamma^{\mathrm{sec}}(E_\gamma) = f_C \int_{E_{\min,C}}^{E_{\max,k}} \left[\frac{\mathrm{d}\sigma_{\mathrm{PE}}(E_\gamma, E)}{\mathrm{d}E} + \frac{\mathrm{d}\sigma_{\mathrm{CS}}(E_\gamma, E)}{\mathrm{d}E} + 2\frac{\mathrm{d}\sigma_{\mathrm{PP}}(E_\gamma, E)}{\mathrm{d}E}\right] \int_{E_{\min,C}}^{E} \frac{N_A}{-\mathrm{d}E'/\mathrm{d}x} \int_{T_{\min,C}}^{T_{\max,C}} \frac{\mathrm{d}\sigma_e(E', T'_C)}{\mathrm{d}T'_C} \times \upsilon_C(T'_C)\,\mathrm{d}T'_C\,\mathrm{d}E'\,\mathrm{d}E, \quad (12)$$

with, f_C = the atom fraction of C in the alloy ($f_C = 0.01$ for Fe–1 at.% C alloy), $T_{\min,C}$ = the minimum C recoil

Table 2
Calculated parameters of interest for gamma ray displacement damage in iron. $T_{\max}$ is the maximum atomic recoil energy for the photoelectric effect (PE), Compton scattering (CS) and pair production (PP)

Gamma ray energy	$T_{\max}$ (eV)			Total damage cross-section (b)	$T_{1/2}$ (eV)
	PE	CS	PP		
1 MeV	77	56	–	2.7×10^{-3}	43
10 MeV	4.2×10^3	4.0×10^3	3.4×10^3	5.9	88
ABWR $\frac{1}{4}T$ spectrum	7.0×10^3	6.7×10^3	6.0×10^3	0.8 [a]	68

[a] Values are the spectral-averaged damage cross-sections determined according to: $\langle\sigma\rangle = \sum_{i=1}^{i_{\max}} \phi_i \sigma(E_\gamma) / \sum_{i=1}^{i_{\max}} \phi_i$

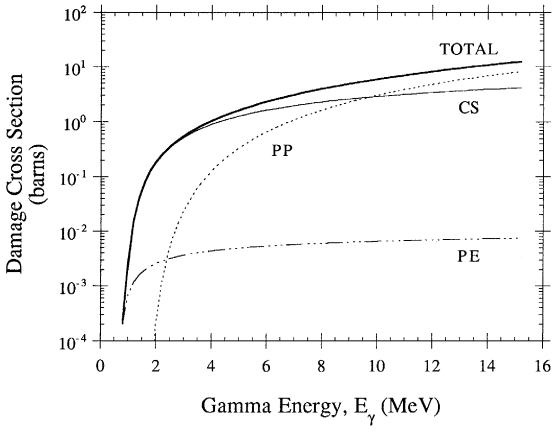

Fig. 2. (a) Displacement damage cross sections in Fe for the photoelectric effect (PE), Compton scattering (CS), pair production (PP) and the total damage cross section (sum of all three interactions) plotted over the energy range of interest for RPVs.

energy capable of displacing an Fe atom, $T_{\max,C}$ = the maximum C recoil energy produced by a gamma-generated electron (found by substituting the C mass, M_C, for M in Eq. (10)), $d\sigma_e(E', T'_C)/dT'_C$ = the differential cross-section for an electron of energy E' to produce a C recoil atom of energy T'_C, $\upsilon_C(T'_C)$ = the damage function for C recoil atoms (i.e., the number of Fe displacements produced by a C recoil of energy T'_C) and $E_{\min,C}$ = the minimum electron energy capable of producing a C recoil atom of energy $T_{\min,C}$ found by solving Eq. (10) for $E_{\min,C}$ after replacing M with M_C, $T_{\max}(E_{\max,k})$ with $T_{\min,C}$ and $E_{\max,k}$ with $E_{\min,C}$.

The value of $T_{\min,C}$ is found from the equation

$$T_{\min,C} = \left[\frac{4MM_C}{(M+M_C)^2}\right]^{-1} T_d. \quad (13)$$

The functional form of the C damage function $\upsilon_C(T'_C)$ was estimated from simulations using the TRIM code [29]. The total displacements/ion were determined for C ion irradiations of a 0.5 μm thick Fe target with $T_d = 40$ eV. Each simulation was performed for 10^5 histories, with incident C ion energies, T'_C, varied between 10^3–2×10^4 eV, to span the anticipated range of C recoil energy for this secondary displacement process. The results could be fit with a linear function of the form

$$\upsilon_C(T'_C) = 2.3 + 4230T'_C. \quad (14)$$

For comparison with the secondary displacement process, the total damage cross-section per target atom for the direct process (i.e., Fe displacement by a gamma generated electron) was found using Eqs. (8) and (9) with Eq. (9) multiplied by a factor of f_{Fe}, the atom fraction of Fe in the alloy ($f_{Fe} = 0.99$ for an Fe–1 at.% C alloy).

Damage cross-sections and $W(T)$ spectra were obtained by numerically integrating Eqs. (6)–(8) and (12), after substituting the appropriate formulae, using Mathematica v. 2.2 software [30]. Calculations were performed for monoenergetic gamma rays of 1 and 10 MeV as well as for an energy spectrum of gammas determined by previous transport calculations [6] at the typically referenced, quarter-thickness ($\frac{1}{4}T$) location of the RPV of the General Electric Advanced Boiling Water Reactor (ABWR) (see Fig. 1).

Table 3
The effects of the secondary displacement process on damage cross sections for monoenergetic gamma ray irradiation of an Fe–1 at.% C alloy. Damage cross-sections consider contributions from the primary damage process–displacement of an Fe atom by a gamma-generated electron — as well as the secondary process–displacement of an Fe atom by a C recoil produced by a gamma-generated electron

Gamma ray energy	Total gamma damage cross-section contribution (b)	
	primary process	secondary process
1 MeV	2.7×10^{-3}	4.0×10^{-4}
10 MeV	5.8	2.4×10^{-2}

3. Results

The calculated results for pure Fe are provided in Figs. 2–4 and Tables 2 and 3. Fig. 2 compares the energy dependence of the calculated damage cross-sections among the three types of gamma interactions. Fig. 3 displays the calculated $W(T)$ spectra for monoenergetic gamma rays and the ABWR gamma energy spectrum. The relative contributions of the three gamma interactions to the integral recoil damage spectra are schematically illustrated in Fig. 4. Table 2 summarizes various calculated results for

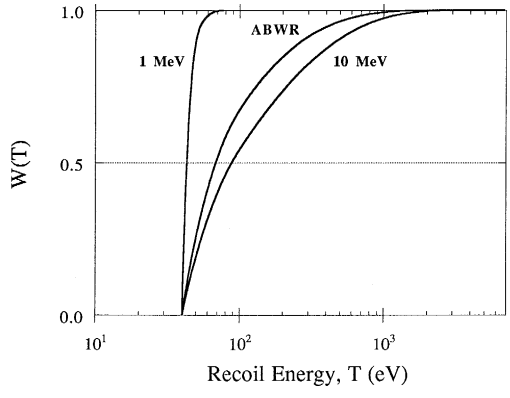

Fig. 3. Integral recoil damage spectra, $W(T)$, calculated for monoenergetic gamma rays and the ABWR $\frac{1}{4}T$ gamma energy spectrum (see Fig. 1) in Fe.

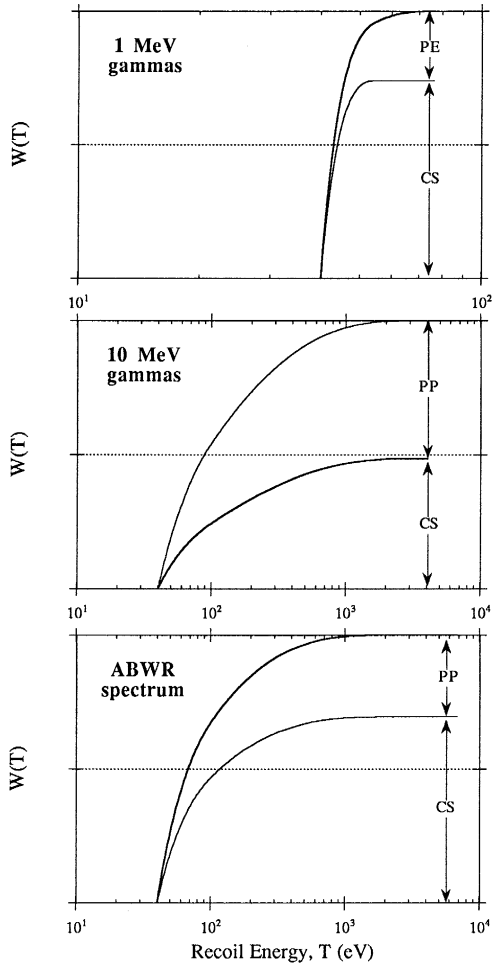

Fig. 4. Relative contributions of the three gamma interactions to the integral recoil damage spectra for 1 MeV gammas (top), 10 MeV gammas (middle), and the ABWR gamma energy spectrum (bottom).

each of the gamma energies of interest, as well as lists the maximum atomic recoil energy produced by each of the three gamma interactions studied. Table 3 gives the results of secondary displacement calculations for an Fe–1 at.% C alloy representative of a steel.

4. Discussion

It is clear from the calculated cross-sections shown in Fig. 2, that damage from CS dominates for most of the gamma energy range of interest in nuclear reactors (i.e., $E_\gamma \leq 14$ MeV). The PE damage cross-section is typically 2–3 orders of magnitude less than that due to CS; however they are comparable at very low energies ≤ 1 MeV. Therefore, consideration should be given to the PE in low-energy gamma ray irradiation environments (for example those produced by Co-60 irradiations). At higher gamma energies (≥ 10 MeV) in Fig. 2, damage due to PP begins to dominate.

The total damage cross-sections calculated in this work compare favorably with those determined previously [4,9,18,19]. For example, considering damage from only CS and PP, Baumann [9] calculated damage cross-sections of 5.2×10^{-3} b and 7.6 b for 1 MeV and 10 MeV gamma rays, respectively. The results of the present work are somewhat smaller: 2.7×10^{-3} and 5.9 b for 1 MeV and 10 MeV gammas, respectively. The difference is explained by the different formulae used to calculate damage from gamma-generated electrons. Baumann's work used Oen's electron damage cross-section calculation results [22] which differ from the present work in two significant ways. First, Oen's calculation used an unmodified Kinchin–Pease damage function (i.e., it lacked the factor of 0.8 found in Eq. (11)) which results in more calculated damage than those used in this work. Second, Oen's calculation used the exact Mott series solution for the differential cross-section, $\mathrm{d}\sigma_e(E', T')/\mathrm{d}T'$, which will result in about 5% greater electron damage (and consequently greater gamma damage) than the McKinley–Feshbach approximation used in the present work [22].

Similarly, damage cross-section comparisons may be made with the work of Rehn and Birtcher [4] in which only displacements from CS were considered. In contrast to the approach of Baumann and the present calculations, their work used an experimentally derived expression for electron displacement damage; i.e., the inner most integration performed over the atomic recoil energy, T', in Eqs. (6)–(8) was replaced by an empirically obtained function dependent on electron energy E'. The function used was derived from Cu data [31] and was therefore deemed representative of a medium-Z metal or alloy such as ferritic steels. Using their approach, Rehn and Birtcher determined damage cross-sections of 3.8×10^{-2} b and 6.6 b for 1 MeV and 10 MeV gamma rays, respectively, which are again somewhat larger than the values calculated in the present study (see Table 2). While for Cu it is obvious that such an approach is superior to using analytical formulae for $\mathrm{d}\sigma_e(E', T')/\mathrm{d}T'$, $\upsilon(T')$ and T_d values to determine recoil damage, for Fe it is debatable whether the absolute magnitudes of the damage cross-sections derived in part from Cu data are more accurate than the analytical formulae.

The contribution of the secondary displacement process to the total damage cross-section for an Fe–1 at.% C alloy is shown in Table 3 for 1 MeV and 10 MeV gamma rays. For 10 MeV gammas the effect is insignificant. For 1 MeV gammas the effect is small, but significant, contributing about 10% of the total displacement damage cross-section. Hence, consideration should be given to secondary displacement phenomena in low-energy gamma ray irradiation environments.

In the case of a spectrum of gamma energies, such as the ABWR spectrum of interest in this work (see Fig. 1),

the subthreshold process increases damage production in a steel by substantially lowering the minimum gamma energy, $E_{\gamma,\min}$, required to produce an Fe displacement. The presence of C in the Fe alloy decreases $E_{\gamma,\min}$ from 0.64 to 0.30 MeV. However, despite the availability of additional damage-producing gamma rays, their contribution to the total defect production is insignificant compared to the contribution from the high energy gammas also present in the spectrum. The total damage cross-sections associated with this low energy gamma flux are orders of magnitude lower than those of the higher energy gamma rays. Hence, as was the case for 10 MeV gamma rays, the subthreshold damage process occurring in steels, for gamma energy spectra characteristic of RPVs, can be reasonably ignored.

Returning to the consideration of gamma damage effects in pure Fe, Fig. 3 shows the calculated $W(T)$ functions for monoenergetic gamma rays and the ABWR gamma spectrum of Fig. 1. Note that the $W(T)$ curves only describe the recoil energy dependence of defect production and, as such, are unaffected by uncertainty in the *absolute* magnitude of the damage cross-section as discussed above. A general characteristic of the $W(T)$ curves in Fig. 3 is that they extend from the threshold displacement energy, T_d, to the maximum recoil energy, T_{max}, which in all cases is defined by the T_{max} produced by the PE (see Table 2). For 1 MeV gammas, displacement damage is generated over a very narrow range of atomic recoil energy (40 eV to 77 eV). For 10 MeV gammas and the ABWR spectrum, damage is produced over a considerably wider range of recoil energies (40 eV to 4.2 keV and 40 eV to 7.0 keV, respectively). Values for the median recoil damage energy, $T_{1/2}$, determined from the energy at which $W(T) = 0.5$, are given in Table 2. Note that the large fluxes of low energy gamma rays in the ABWR spectrum result in a $W(T)$ curve that is somewhat 'softer', with a smaller $T_{1/2}$ value, than the 10 MeV gamma rays.

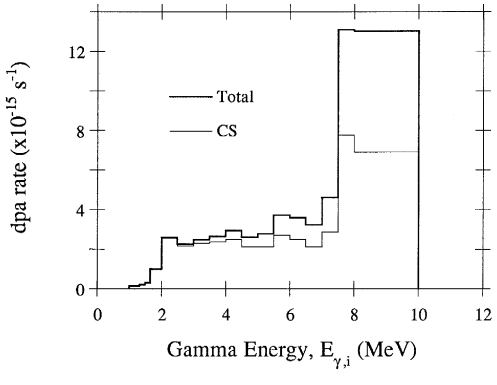

Fig. 5. Spectral contribution of gamma interactions to defect production rates for the ABWR spectrum shown in Fig. 1. The PE contributes negligibly to the dpa rate at all gamma energies. The PP contribution is the difference between the total curve and the CS curve.

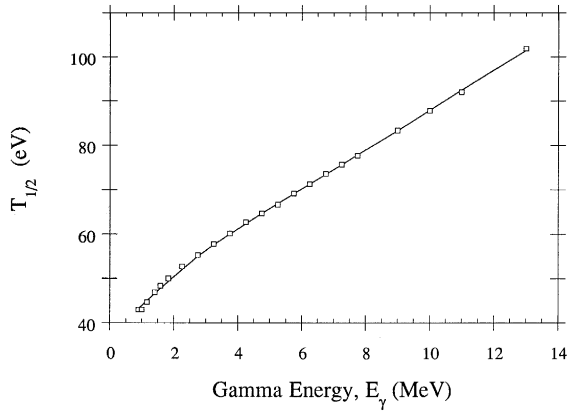

Fig. 6. Median recoil damage energy calculated as a function of the gamma ray energy.

The fractional contributions of the three gamma interactions to the total $W(T)$ curves are displayed in Fig. 4. For 1 MeV gamma rays (top graph in Fig. 4), about 75% of the damage is contributed by CS with the PE contributing the remainder. Note that PP is not operative since the gamma energy is less than the required $2m_ec^2$. For the 10 MeV gamma rays (middle graph in Fig. 4), the contribution from the PE is negligible with CS and PP contributing about equally to the damage at this energy. For the ABWR gamma spectrum (bottom graph in Fig. 4), CS contributes about 70%, with PP contributing the remainder. The increased effect of CS in this case, relative to that observed for 10 MeV gammas, is a result of the large fluxes of lower energy gamma rays present in the ABWR spectrum (see Fig. 1).

In the case of the ABWR, it is of interest to consider the spectral dpa rate contributions of each of the gamma

Table 4
Comparison of median recoil damage energies, $T_{1/2}$, and maximum recoil energies, T_{max}, produced by irradiation with various 1 MeV particles in Fe. Ion $T_{1/2}$ values determined from $W(T)$ curves calculated using a modified version of the TRIM code [a] [29]. Neutron value determined from a $W(T)$ curve calculated using a hard-sphere scattering cross-section. Electron value obtained from a $W(T)$ curve calculated using the McKinley–Feshbach differential cross section [19,20]

1 MeV particle	$T_{1/2}$ (eV)	T_{max} (eV)
Gamma ray	43	77
Electron	49	78
He-ion	2300	250 000
Neutron	49 000	69 500
Xe-ion	89 000	840 000

[a] TRIM calculations performed for one million histories using $T_d = 40$ eV and an Fe target thickness of 100 Å for He-ions and 10 Å for Xe-ions. Thicknesses chosen to insure a maximum of one ion interaction with the target per history simulated.

interactions at the $\frac{1}{4}T$ location of the RPV. Fig. 5 shows these dpa rate contributions determined using the gamma flux spectrum from Fig. 1 and the gamma damage cross-sections from Fig. 2. The PE contributes negligibly to defect production in this spectrum and can be reasonably ignored. The contribution of PP in the figure is the difference between the total dpa rate curve and the CS dpa rate curve. Above 3 MeV, PP begins to contribute increasingly to the dpa rate, equaling in magnitude that produced by CS in the energy range of 7.5–10 MeV, where a large fraction of the defect production is produced. Clearly, it is necessary to consider PP displacement damage for such RPV spectra if an accuracy of better than 30% is to be attained.

In the process of evaluating the ABWR spectral $W(T)$ it was possible to extract $W(T)$ curves and corresponding $T_{1/2}$ values for each individual gamma energy bin comprising the spectrum. The resulting $T_{1/2}$ values, along with those for the monoenergetic gamma rays from Table 2, are plotted as a function of gamma ray energy in Fig. 6. Using this energy dependence, it is possible to provide practical estimate of the median recoil damage energy for other discretized gamma ray energy spectra, ϕ_i. Defining the energy dependence displayed in Fig. 6 as $T_{1/2}(E_{\gamma,i})$, a spectral-averaged median recoil energy value, $\langle T_{1/2}\rangle$, may be evaluated as

$$\langle T_{1/2}\rangle = \frac{\sum_{i=1}^{i_{max}} \phi_i T_{1/2}(E_{\gamma,i})}{\sum_{i=1}^{i_{max}} \phi_i}. \quad (15)$$

It is clear from the preceding discussion that gammas produce a soft recoil damage spectrum. This fact is reinforced by Table 4, which compares $T_{1/2}$ values and maximum recoil energies in Fe produced by various 1 MeV particles, including the gamma ray result obtained in this calculation. The median recoil damage energy for gammas, while of a similar magnitude as 1 MeV electrons, is substantially less than that for all the other particles. The $T_{1/2}$ is about three orders of magnitude less than that for a 1 MeV neutron.

As described in Section 1 it is the comparison with neutrons which is of particular interest for interpreting the relative contribution of gamma ray produced defects to the microstructural evolution causing RPV embrittlement. Fig. 7 displays the $W(T)$ spectra for both gamma rays and neutrons (of all energies) at the $\frac{1}{4}T$ location of the GE ABWR. The neutron spectrum was obtained from SPECTER calculations [10,11] using as input the $\frac{1}{4}T$ neutron flux energy spectrum. As seen in Fig. 7, the neutron irradiation produces defects at considerably higher recoil energies than the gamma rays. The median recoil damage energy for the ABWR gamma spectrum is three orders of magnitude less than that for the neutron spectrum consistent with the large difference observed in the monoenergetic particle comparison above.

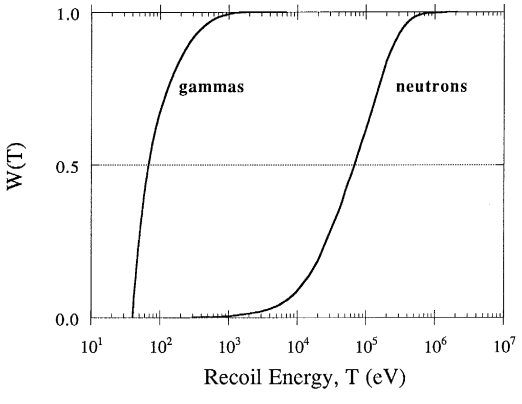

Fig. 7. $W(T)$ spectra determined for gamma ray and neutron flux energy spectra at the $\frac{1}{4}T$ location of the ABWR.

5. Conclusions

Damage cross-section calculations show that defect production by 10 MeV gamma rays, and by gammas with a spectrum of energies characteristic of RPVs, is caused primarily by gamma-generated electrons and positrons from Compton scattering and pair-production. In low-energy (≤ 1 MeV) gamma irradiations (similar to Co-60 irradiations) consideration must also be given to defect production from the photoelectric effect. Secondary displacement damage, produced from recoils of light alloy elements such as carbon in steel, is insignificant in gamma environments of interest to RPVs but should be considered in low-energy gamma irradiations.

Integral recoil damage spectra, $W(T)$, in iron indicate that damage is produced at very low atomic recoil energies during gamma irradiation, with median recoil damage energies, $T_{1/2}$, typically less than 100 eV. The $W(T)$ spectra for gamma rays are considerably 'softer' than those produced by other types of irradiation. This contrast is particularly notable in comparison with neutron irradiation where the $T_{1/2}$ values for gamma irradiations of iron are three orders of magnitude smaller than corresponding neutron values. Recognition of the substantial difference in the nature of defect production between these two types of irradiation should prove useful in evaluating and understanding the contribution of gamma rays to radiation embrittlement of reactor pressure vessel steels.

Acknowledgements

Suggestions and comments on this work offered by R.C. Birtcher, R. Gold, L. Rehn, T. Daulton, L. Greenwood, A. Motta, M. Giacobbe, D. Narayanaswamy and P. Liu are gratefully acknowledged.

References

[1] R.A. Dugdale, in: Report of the Conf. on Defects in Crystalline Solids, Bristol, 1954 (Phys. Soc., London, 1955) p. 246.
[2] D.O. Thompson and D.K. Holmes, J. Phys. Chem. Solids 1 (1957) 275.
[3] R.E. Larsen and A.C. Damask, Acta Metall. 12 (1964) 1131.
[4] L.E. Rehn and R.C. Birtcher, J. Nucl. Mater. 205 (1993) 31.
[5] D.E. Alexander and L.E. Rehn, J. Nucl. Mater. 209 (1994) 212.
[6] D.E. Alexander and L.E. Rehn, J. Nucl. Mater. 217 (1994) 213.
[7] K. Farrell, S.T. Mahmood, R.E. Stoller and L.K. Mansur, J. Nucl. Mater. 210 (1994) 268.
[8] I. Remec, J.A. Wang, F.B.K. Kam and K. Farrell, J. Nucl. Mater. 217 (1994) 258.
[9] N.P. Baumann, in: 7th ASTM-Euratom Symposium on Reactor Dosimetry, eds. G. Tsotridis, R. Dierckx and P. D'Hondt (Kluwer Academic, Boston, MA, 1992) p. 689.
[10] L.R. Greenwood and R.K. Smither, Argonne National Laboratory, ANL/FPP/TM-197, 1985.
[11] GE ABWR SPECTER output data supplied by L.R. Greenwood, Battelle Pacific Northwest Laboratory.
[12] W.J. Phythian, R.E. Stoller, A.J.E. Foreman, A.F. Calder and D.J. Bacon, J. Nucl. Mater. 223 (1995) 245.
[13] D.J. Bacon and T. Diaz del la Rubia, J. Nucl. Mater. 216 (1994) 275.
[14] L.E. Rehn and H. Wiedersich, Mater. Sci. Forum 97–99 (1992) 43.
[15] H. Wollenberger, V. Naundorf and M.-P. Macht, in: Diffusion Processes in Nuclear Materials, ed. R.P. Agarwala (Elsevier Science, Amsterdam, 1992) p. 201.
[16] R.S. Averback, J. Nucl. Mater. 216 (1994) 49.
[17] W. Schilling and H. Ullmaier, in: Nuclear Materials, ed. B.R.T. Frost, Vol. 10B, from the series, Materials Science and Technology, eds. R.W. Cahn, P. Haasen and E.J. Kramer (VCH, Weinheim, 1994) p. 190.
[18] O.S. Oen and D.K. Holmes, J. Appl. Phys. 30 (1959) 1289.
[19] G.J. Dienes and G.H. Vineyard, Radiation Effects in Solids (Interscience, New York, 1957) p. 50.
[20] A.B. Chilton, J.K. Shultis and R.E. Faw, Principles of Radiation Shielding (Prentice Hall, Englewood Cliffs, NJ, 1984).
[21] F. Seitz and J.S. Koehler, in: Solid State Physics, eds. F. Seitz and D. Turnbull, Vol. 2 (Academic Press, New York, 1956) p. 305.
[22] O.S. Oen, Oak Ridge National Laboratory, ORNL-4897 (1973).
[23] O.R. Frisch, ed., The Nuclear Handbook (George Newnes, 1958) pp. 8–6.
[24] Standard Practice for Neutron Radiation Damage Simulation by Charged-Particle Irradiation E 521-83, ASTM Standards, Section 12 (1986).
[25] E.U. Condon and H. Odishaw, eds., Eq. 8.14 in Handbook of Physics (McGraw-Hill, New York, 1967) pp. 7–131.
[26] D.E. Gray, ed., Eq. (8e-21) in American Institute of Physics Handbook (McGraw-Hill, New York, 1972) pp. 8–196.
[27] P.V.C. Hough, Phys. Rev. 74 (1948) 266.
[28] P.G. Regnier, N.Q. Lam and K.H. Westmacott, J. Nucl. Mater. 115 (1983) 286.
[29] J.P. Biersack and L.G. Haggmark, Nucl. Instrum. Methods 174 (1980) 257.
[30] Mathematica, Wolfram Research Inc. (1993).
[31] A.C. Baily, thesis, Northwestern University (1986).